Preparation, crystal structure, heat capacity, magnetism, and the magnetocaloric effect of $Pr_5Ni_{1.9}Si_3$ and PrNi

A. O. Pecharsky,[1] Yu. Mozharivskyj,[1] K. W. Dennis,[1] K. A. Gschneidner, Jr.,[1,2] R. W. McCallum,[1,2] G. J. Miller,[1,3] and V. K. Pecharsky[1,2,*]

[1]*Materials and Engineering Physics Program, Ames Laboratory, Iowa State University, Ames, Iowa 50011-3020, USA*

[2]*Department of Materials Science and Engineering, Iowa State University, Ames, Iowa 50011-3114, USA*

[3]*Department of Chemistry, Iowa State University, Ames, Iowa 50011-3111, USA*

(Received 11 July 2003; published 29 October 2003)

Single-phase $Pr_5Ni_{1.9}Si_3$ and PrNi were prepared and characterized by using differential thermal analysis, single crystal, and powder x-ray diffraction. Their thermal and magnetic properties were studied by measuring heat capacity as a function of temperature in magnetic fields up to 100 kOe and magnetization as a function of magnetic field up to 50 kOe over the temperature range from 5 to 400 K. $Pr_5Ni_{1.9}Si_3$ orders magnetically at 50 K, and it undergoes a second transition at 25 K. As inferred from the behavior of the magnetization and magnetocaloric effect (MCE), both ferromagnetic and antiferromagnetic components are present in the magnetic ground state of the material. The heat capacity and magnetocaloric effect of PrNi confirm that it orders ferromagnetically at 19 K. Both $Pr_5Ni_{1.9}Si_3$ and PrNi exhibit moderate magnetocaloric effects. The maximum MCE for $Pr_5Ni_{1.9}Si_3$ is 3.4 K and it is observed at 50 K for a magnetic field change from 0 to 75 kOe. The maximum MCE for PrNi is 4.2 K, which occurs at 19 K for a magnetic field change from 0 to 100 kOe.

DOI: 10.1103/PhysRevB.68.134452 PACS number(s): 75.30.Sg, 75.50.−y, 61.66.Dk

I. INTRODUCTION

A considerable number of ternary intermetallic compounds form in *R*-*M*-Si systems, where *R* is rare earth and *M* is transition metal. Many of these intermetallic phases possess different but related crystal structures, and as a result, their physical properties may, and often do, vary systematically. On the one hand, diverse phase relationships reflect the complexity of chemical interactions between $4f$ and $3d$-$5d$ metals with semimetallic silicon, thus enabling one to finely tune the physical properties of a system via controlled adjustments of the chemical composition, which result in systematic variations of the crystal structure. On the other hand, detailed studies of physical behavior of many *R*-*M*-Si intermetallics may be complicated and sometimes are nearly impossible due to considerable difficulties in the preparation of single-phase samples.

The ternary Pr-Ni-Si system is one of the examples, where approximately 20 individual intermetallic phases have been reported in the literature, but no ternary phase diagram or at least an isothermal section of the diagram has been constructed to date. The most recent summary of the ternary phases known to form in the Pr-Ni-Si system and their crystal structures was given by Rogl in 1987.[1] Intriguing structural relationships exist between several intermetallic phases found in this system in the range of concentrations from 45 to 55 at.% Pr and from 15 to 40 at.% Ni. These are $Pr_6Ni_2Si_3$, Pr_2NiSi, $Pr_{15}Ni_7Si_{10}$, and $Pr_{15}Ni_4Si_{13}$. All four compounds are hexagonal, and they crystallize in the space group $P6_3/m$. $Pr_6Ni_2Si_3$ belongs to the $Ce_6Ni_2Si_3$-type structure with lattice parameters $a=12.005(5)$ and $c=4.273(2)$ Å.[2] Pr_2NiSi has the same crystal structure as Ce_2NiSi, and its lattice parameters are $a=16.05(1)$ and $c=4.302(5)$ Å.[3] $Pr_{15}Ni_7Si_{10}$ has its own type of crystal structure with lattice parameters $a=19.881(1)$ and $c=4.2554(3)$ Å.[4] $Pr_{15}Ni_4Si_{13}$ was reported to be isostructural with $Ce_{15}Ni_4Si_{13}$, and unit cell dimensions of the former are $a=20.19$ and $c=4.297$ Å.[5] Considering the identical stoichiometry with respect to *R* and (Ni+Si) atoms and the similarity of the unit cell dimensions, the latter two alloys with praseodymium are likely to represent two different compositions from the same phase region.

According to Bodak and Gladyshevskii,[6] the Ce_2NiSi-, $Ce_6Ni_2Si_3$-, and $Ce_{15}Ni_4Si_{13}$-type structures are closely related to one another. They belong to the two-dimensional homologous series based on several simple metallic structures, i.e., AlB_2, α-Fe, and NiAs. As illustrated in Fig. 1, the three structures differ from one another in the configuration of the bases of the complex trigonal prismatic columns, which are limited in the *XY* plane and are infinite along the *Z* axis. The building blocks of these columns are the small trigonal prisms formed by *R* (e.g., Ce) atoms, which are filled with either Si or Ni atoms or by statistical mixtures thereof. The stoichiometry of each member of this homologous series may be derived from $R_{n^2+3n+2}(Ni,Si)_{2n^2+2}$, where *n* is the number of small trigonal prisms that fit along the side of the complex trigonal prismatic column; compounds with the value of *n* varying from 2 to 4 have been reported for a range of different *R* elements. For example, for $Ce_{15}Ni_4Si_{13}$, $n=4$, and its stoichiometry is $R_{30}(Ni,Si)_{34}=R_{15}(Ni,Si)_{17}$. Bonding among the atoms that belong to the column is likely to be different from that between the columns, and therefore, a systematic dependence of physical and especially magnetic properties of these compounds on their chemical composition and structure may be expected.

The availability of complex and clearly anisotropic crystal structures similar to the $R_{n^2+3n+2}(Ni,Si)_{2n^2+2}$ homologous series, therefore, provides a way to better understand the relationships between chemical composition, crystal structure, and physical properties of metallic materials. In this paper,

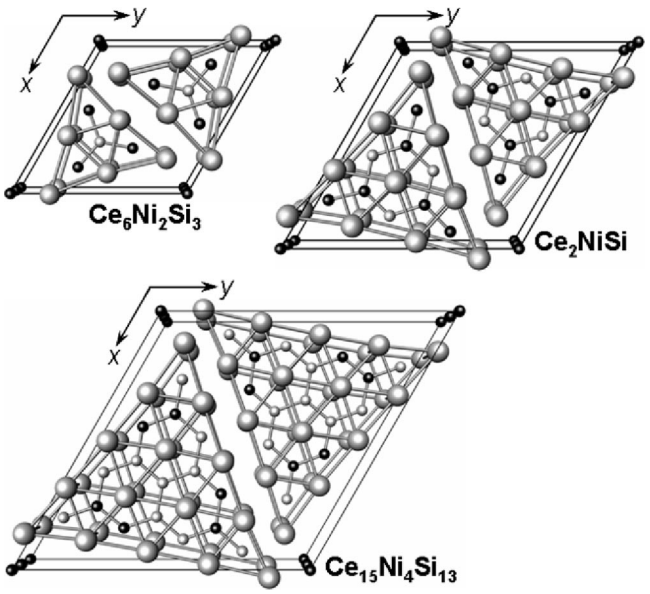

FIG. 1. Perspective views of the unit cells of $Ce_6Ni_2Si_3$, Ce_2NiSi, and $Ce_{15}Ni_4Si_{13}$ structure types. Ce (R) atoms are large gray, Ni and Ni+Si atoms are small black, and Si atoms are small gray spheres. The Z axis is normal to the plane of the paper.

we report on the preparation, crystal structure, and basic thermal and magnetic properties of the ''Pr_2NiSi'' compound, which is the member of the same series with $n=3$. In addition to this ternary silicide, we also prepared binary PrNi and studied its heat capacity and magnetocaloric effect.

II. SAMPLE PREPARATION AND CHARACTERIZATION

The polycrystalline Pr_2NiSi was prepared by arc melting in an argon atmosphere from high-purity components. The Pr metal was obtained from the Materials Preparation Center of the Ames Laboratory and was 99.9+ at. % pure. The major impurities in Pr were F-222, O-203, Si-120, N-101, Fe-6.8, and Nd-2.2 (all numbers are in parts per million atomic). The Ni (99.88 at. % pure) and Si (99.99 at. % pure) were purchased from commercial vendors. Pr_2NiSi was remelted 6 times to ensure its homogeneity; after each melting, the alloy button was turned over and melted again. According to x-ray powder diffraction analysis (Scintag powder diffractometer, Cu $K\alpha$ radiation, $20° \leqslant 2\theta \leqslant 90°$) coupled with Rietveld refinement, the as-arc-melted Pr_2NiSi contained two phases. They were identified as $\sim Pr_2NiSi$ (the majority phase), belonging to the hexagonal Ce_2NiSi-type structure, and PrNi (the minority phase), which has the orthorhombic CrB-type crystal structure. Samples of Pr_2NiSi were heat treated at different temperatures from 500 to 680 °C for different periods of time ranging from 1 day to 1 week. In each case, the alloy remained a mixture of two phases according to x-ray diffraction, although their contents in the alloy varied as a result of heat treatments. The presence of about 20 vol. % of PrNi was also confirmed by metallography using a sample, which was heat treated at 680 °C for 4 days. The metallographic examination was carried out after the surface of the alloy was polished using different grades of aluminum oxide powders suspended in water with a final particle size of 0.03 μm. The surface was self-etched during the polishing without using any additional chemicals.

The persistence of the PrNi phase after various heat treatments was a solid indicator that the Pr_2NiSi stoichiometry, which was reported in the literature, may be not quite accurate. Therefore, in an attempt to determine the correct chemical composition of the majority phase, we carried out a complete structural investigation using two single crystals extracted from the alloy heat treated at 680 °C for 4 days. The single-crystal x-ray diffraction experiments were carried out on a Bruker SMART Apex charge-coupled devices (CCD) diffractometer using Mo $K\alpha$ radiation. The diffraction data were collected at room temperature in full reciprocal sphere to $2\theta_{max}=57°$. Unit cell dimensions were refined using all observed Bragg reflections. The absorption correction was accounted using SADABS (Ref. 7) employing Bragg reflections with $I/\sigma(I)>3$. The crystal structure was solved by direct methods and refined by using the least-squares technique based on F^2. Population parameters of Ni and Si atoms located in different sites were included as free variables during the refinement to determine chemical compositions of the crystals.

The chemical composition of the majority phase, determined from the single crystal diffraction experiments, was found to be $Pr_5Ni_{1.9}Si_3$. Therefore, the alloy with this stoichiometry was prepared by arc melting following the same procedure as described above. The x-ray powder diffraction pattern of as-arc-melted $Pr_5Ni_{1.9}Si_3$ was again indicative of more than one phase with the majority phase belonging to the hexagonal Ce_2NiSi-type structure. Other phases in small quantities were detected but not identified. After heat treating the alloy at 600 °C for 5 days, its x-ray powder diffraction pattern showed only a single phase and metallographic examination showed less than 2 vol. % of the second phase in the alloy. This second phase was identified as PrNi using scanning electron microscopy and energy dispersive spectroscopy.

Since an identifiable amount of PrNi was present in the essentially pure heat-treated $Pr_5Ni_{1.9}Si_3$, we also prepared the former using the same technique and starting components as described above. The x-ray powder diffraction pattern of the as-arc-melted PrNi contained a major phase with the orthorhombic CrB-type crystal structure.[8] $PrNi_2$ with $MgCu_2$-type crystal structure[9] was present as an impurity phase. Since according to the corresponding phase diagram[10] PrNi melts congruently, we verified the absence of defects on Ni sites by examining the crystal structure of the material using single-crystal x-ray diffraction employing a specimen extracted from the as arc-melted piece of the alloy. Single-phase PrNi was then obtained by heat treating a sample at 600 °C for 5 days. Both the x-ray powder diffraction pattern and metallography of the heat treated PrNi showed it to be a single-phase material.

The heat-treated samples of $Pr_5Ni_{1.9}Si_3$ and PrNi were used to measure their magnetic properties and heat capacities, and evaluate their magnetocaloric effects. Magnetization was measured using a Quantum Design magnetometer between 5 and 400 K in magnetic fields ranging from 0 to 50

TABLE I. Crystallographic data and structure refinement for $Pr_5Ni_{1.9}Si_3$.

Refined stoichiometry	$Pr_5Ni_{1.9}Si_3$
Structure type	Ce_2NiSi
Temperature of the experiment	293(2) K
Wavelength	0.71073 Å
Space group	$P6_3/m$
Unit cell dimensions	$a=15.9268(8)$, $c=4.2553(3)$ Å
Unit cell volume	934.80(9) Å^3
Number of formula units in the cell, Z	4
Calculated density	6.398 g/cm^3
Absorption coefficient	29.578 mm^{-1}
F(000)	1561
Data collection range 2θ	2.96°–56.64°
Index ranges	$-20<h<20$, $-21<k<21$, $-5<l<5$
Reflections collected	8186
Independent reflections	860 ($R_{int}=0.0292$)
Completeness to $2\theta=56.64°$	97.4%
Refinement method	Full matrix least squares on F^2
Data/restraints/parameters	860/0/45
Goodness of fit on F^2	1.102
Final R indices [$I>2\sigma(I)$]	$R_1=0.0173$, $wR_2=0.0330$
R indices (all data)	$R_1=0.0200$, $wR_2=0.0336$
Extinction coefficient	0.00027(3)
Largest difference peak and hole	0.973e and $-0.962e$ Å^{-3}

kOe. The heat capacities were measured in a semiadiabatic heat pulse calorimeter[11] between ~3.5 and 350 K in constant magnetic fields of 0, 20, 50, 75, and 100 kOe. The magnetocaloric effect (MCE) was calculated from the heat capacity measurements as described in Ref. 12.

III. EXPERIMENTAL RESULTS AND DISCUSSION

A. Crystallography of $Pr_5Ni_{1.9}Si_3$ and PrNi

The crystallographic data of both the $Pr_5Ni_{1.9}Si_3$ and PrNi compounds, as determined from the single-crystal x-ray diffraction analysis, are listed in Tables I–IV. Short distances between the Ni atoms located in $4(e)$ and $2(a)$ sites of the $Pr_5Ni_{1.9}Si_3$ structure (Table II) require partial occupancies of these sites with the total number of Ni atoms in both sites not to exceed 2 due to geometrical constrains. Unrestrained refinement of the occupancies of Ni2 and Ni3 resulted in slightly less than two Ni atoms total, i.e., 1.62(8) Ni atoms occupying positions located on the twofold axis, which coincides with the 6_3 axis. Refinement of the occupancies of other sites did not result in statistically significant deviations from unity, and therefore, all remaining sites appear to be fully occupied. A second crystal was extracted from the same alloy and it was also examined using single-crystal x-ray diffraction. The results, including refined occupancies of $4(e)$ and $2(a)$ sites, were identical with the first crystal to within two standard deviations, and therefore, we conclude that despite considerable defects, this intermetallic compounds forms at a fixed chemical composition. The resulting stoichiometry of the formula unit is $Pr_5Ni_{1.91\pm0.02}Si_3$, and the crystal structure of $Pr_5Ni_{1.9}Si_3$, including Ni2 and Ni3 atoms, is shown in Fig. 2. This illustration highlights the presence of complex trigonal prismatic assemblies build from small trigonal prisms with Pr atoms in the corners. The prisms are filled with either Si or Ni atoms. The columns are infinite along the Z axis and they are limited within the XY plane, containing nine small trigonal prisms in the base of each column.

The observed and calculated powder diffraction patterns of $Pr_5Ni_{1.9}Si_3$ are shown in Fig. 3 and those of PrNi in Fig. 4. The unit cell dimensions determined from Rietveld refinement based on powder data, i.e., $a=15.9276(6)$ and $c=4.2549(2)$ Å for $Pr_5Ni_{1.9}Si_3$, are the same within the experimental error limits as those obtained from the single-crystal measurements: see Table I. The values for PrNi [$a=3.8234(6)$, $b=10.509(1)$, $c=4.3583(3)$ Å], however, are slightly different from those obtained from the single-crystal experiment: see Table III. The small but systematic discrepancies in the latter case could be due to the fact that the powder diffraction technique usually yields more accurate unit cell dimensions when compared to the single-crystal diffraction data. The difference, however, may be indicative of a slight deviation in the Pr to Ni ratio from unity in one or both samples: i.e., PrNi may have variable stoichiometry and exist over a small range of concentrations.

TABLE II. Atomic coordinates, occupancies, and equivalent isotropic displacement parameters (Å^2) for $Pr_5Ni_{1.9}Si_3$.

Atom	Site	Occupancy	x/a	y/b	z/c	U_{eq}[a]
Pr1	$6(h)$	1.00	0.01017(2)	0.18033(3)	1/4	0.0149(1)
Pr2	$6(h)$	1.00	0.39923(2)	0.26302(2)	1/4	0.0114(4)
Pr3	$6(h)$	1.00	0.45425(2)	0.06747(2)	1/4	0.0113(1)
Pr4	$2(d)$	1.00	2/3	1/3	1/4	0.0113(1)
Ni1	$6(h)$	1.00	0.28184(5)	0.49788(5)	1/4	0.0125(2)
Ni2	$4(e)$	0.246(9)	0	0	0.084(1)	0.02(2)
Ni3	$2(a)$	0.32(2)	0	0	1/4	0.02(2)
Si1	$6(h)$	1.00	0.1647(1)	0.5499(1)	1/4	0.0119(3)
Si2	$6(h)$	1.00	0.2316(1)	0.3256(1)	1/4	0.0120(3)

[a] U_{eq} is defined as one-third of the trace of the orthogonalized U_{ij} tensor.

TABLE III. Crystallographic data and structure refinement for PrNi.

Empirical formula	PrNi
Structure type	CrB
Temperature of experiment	293(2) K
Wavelength	0.71073 Å
Space group	*Cmcm*
Unit cell dimensions	$a=3.8307(9)$, $b=10.543(2)$, $c=4.369(1)$ Å
Unit cell volume	176.44(7) Å^3
Number of formula units per cell, Z	4
Calculated density	7.515 g/cm^3
Data collection range 2θ	7.74°–55.88°
Index ranges	$-4<h<4$, $-13<k<13$, $-5<l<5$
Reflections collected	711
Independent reflections	133 ($R_{\text{int}}=0.0213$)
Completeness to $2\theta=55.88°$	97.1%
Refinement method	Full matrix least squares on F^2
Data/restraints/parameters	133/0/9
Goodness of fit on F^2	1.169
Final R indices $[I>2\sigma(I)]$	$R_1=0.0156$, $wR_2=0.0355$
R indices (all data)	$R_1=0.0158$, $wR_2=0.0357$
Largest difference peak and hole	0.940e and $-1.083e$ Å^{-3}

B. Differential thermal analysis of $Pr_5Ni_{1.9}Si_3$

Differential thermal analysis (DTA) of an annealed $Pr_5Ni_{1.9}Si_3$ sample (see Fig. 5) displays a complex melting behavior. A small endothermic peak with an onset at 660 °C contains approximately 2% of the total area under the endothermic peaks, which corresponds to the amount of the PrNi impurity. The total energy in this peak is consistent with either a solid-state transformation or a eutectic melting involving a small amount of one or two additional phases. Further studies are required to determine the origin of this peak. The large and sharp endotherm with an onset of 998 °C is consistent with a peritectic decomposition of the $Pr_5Ni_{1.9}Si_3$ phase at this temperature, while the endotherm with an onset at 1085 °C appears to contain at least two and possibly three melting events.

From the DTA, it appears that solidification of $Pr_5Ni_{1.9}Si_3$ occurs through a cascade of peritectic reactions. As a result, extended annealing is required in order to prepare a high-quality sample. Ongoing investigations of the relevant part of the Pr-Ni-Si phase diagram indicate that the liquids, which form, are highly reactive with most commonly used crucible materials, and thus special care is required during annealing to avoid contamination from the container.

C. Heat capacity and magnetocaloric effect of $Pr_5Ni_{1.9}Si_3$ and PrNi

Figure 6 shows the heat capacity of $Pr_5Ni_{1.9}Si_3$ as a function of temperature measured in 0, 20, 50, and 75 kOe magnetic fields. A distinct λ-type anomaly is observed in zero magnetic field at ~50 K and its behavior as the field increases clearly indicates that the corresponding second-order phase transition is magnetic in origin. Assuming that Ni is nonmagnetic in this intermetallic phase, which is typical for the majority of other R-Ni-Si compounds, the magnetic ordering in the Pr sublattice occurs at quite high temperature, especially considering that crystal field splittings from the singlet ground states inhibit spontaneous magnetic ordering in pure Pr; the latter does not order magnetically down to 2 K.[13] Above 50 K, the heat capacity shows conventional behavior saturating at $\sim 3R$ around 200 K.

In addition to the major λ-type peak mentioned above, a small cusplike anomaly is observed at ~25 K. The latter is too strong to be due to a magnetic ordering of the PrNi impurity (less than 2 vol. % total); furthermore, PrNi was reported (also see below) to order ferromagnetically at 20 K.[14] The ~25 K cusp shifts towards lower temperature and remains noticeable in a 20 kOe magnetic field, but it is completely suppressed by 50 kOe and higher fields. This behavior is consistent with the development of an antiferromagnetic component in the magnetic interactions at 25 K and indicates that the antiferromagnetism in $Pr_5Ni_{1.9}Si_3$ can be quenched by magnetic fields greater than 20 kOe.

Below ~8 K, the C/T vs T^2 plot shows a linear behavior and the least-squares fit to $C=\gamma T+\beta T^3$ results in the electronic heat capacity coefficient $\gamma=8.0(9)$ mJ/g atom K, and the Debye temperature $\Theta_D=144(2)$ K. Although these values may be slightly affected by magnetic contributions to the heat capacity, the electronic heat capacity coefficient indicates a normal density of states at the Fermi level.

The magnetocaloric effect of $Pr_5Ni_{1.9}Si_3$, calculated from the heat capacity data in terms of the magnetic entropy change $(-\Delta S_M)$ and the adiabatic temperature change (ΔT_{ad}), is shown in Figs. 7(a) and 7(b), respectively. The MCE peaks at ~50 K and its behavior is indicative of ferromagnetic coupling in the Pr sublattice. Clearly, there is a negative component of the MCE below ~20 K, which reflects an antiferromagnetic component developing as the temperature is lowered. It is, therefore, feasible that the cusp in heat capacity observed at ~25 K in zero magnetic field

TABLE IV. Atomic coordinates, occupancies, and equivalent isotropic displacement parameters (Å^2) for PrNi.

Atom	Site	Occupancy	x/a	y/b	z/c	U_{eq}[a]
Pr	4(c)	1.00	0	0.36178(4)	3/4	0.0131(2)
Ni	4(c)	1.00	0	0.0724(1)	3/4	0.0177(3)

[a]U_{eq} is defined as one-third of the trace of the orthogonalized U_{ij} tensor.

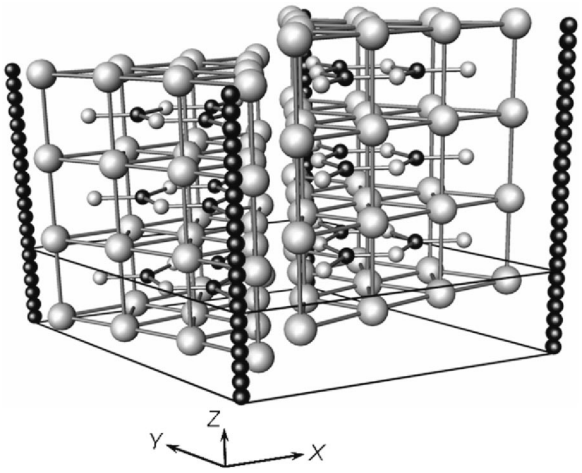

FIG. 2. Perspective view illustrating complex trigonal prismatic arrangement in the crystal structure of $Pr_5Ni_{1.9}Si_3$. The Pr atoms are large gray, the Ni atoms are small black, and the Si atoms are shown as small gray spheres. One unit cell is delineated using thin solid lines.

could be due to a spin reorientation transition, which occurs in $Pr_5Ni_{1.9}Si_3$ at this temperature. The cusp in the heat capacity (Fig. 6, inset) and the negative MCE (Fig. 7) around 25 K are consistent with the magnetization measurements: see below. The magnetocaloric effect in this compound is quite low, which is expected considering the low magnetic moment of Pr when compared, for example, to heavy lanthanides such as Gd, Tb, Dy, and Er.

The heat capacity of PrNi as a function of temperature measured in 0, 20, 50, 75, and 100 kOe magnetic fields is shown in Fig. 8. Similar to that of the upper-temperature transition in $Pr_5Ni_{1.9}Si_3$, PrNi undergoes a second-order phase transformation from a ferromagnetic to a paramagnetic state on heating. The transition temperature obtained from

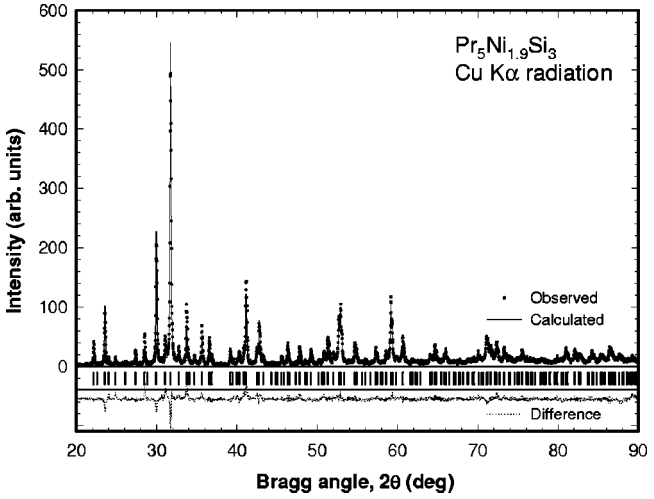

FIG. 3. Observed and calculated x-ray powder diffraction patterns of $Pr_5Ni_{1.9}Si_3$ heat treated at 600 °C for 5 days. Vertical bars at the bottom of the plot indicate calculated positions of Bragg peaks. The difference between the observed and calculated patterns is also shown at the bottom of the plot.

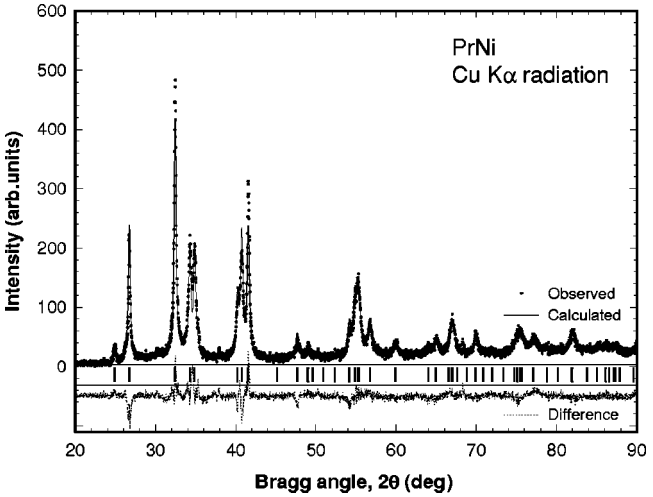

FIG. 4. Observed and calculated x-ray powder diffraction patterns of PrNi heat treated at 600 °C for 5 days. Vertical bars at the bottom of the plot indicate calculated positions of Bragg peaks. The difference between the observed and calculated patterns is also shown at the bottom of the plot.

the zero-field heat capacity data (19 K) is in an excellent agreement with that deduced earlier from magnetization measurements.[14] The magnetic contribution to the heat capacity remains large down to the lowest temperature of the experiment ($\sim$4 K). As a result, it was impossible to obtain reasonable fits of the data to determine the electronic heat capacity and the Debye temperature for this material even after including the spin-wave contribution for a simple ferromagnetic material, where the magnetic heat capacity is given as $C_m = DT^{3/2}$,[15] or for an anisotropic ferromagnet, in which $C_m = D^{3/2}\exp(-\Delta/kT)$.[16] The magnetocaloric effect of PrNi is shown in Figs. 9(a) and 9(b). The caretlike behavior is typical of a conventional ferromagnet, and the MCE is comparable but slightly larger than that observed in $Pr_5Ni_{1.9}Si_3$. The latter is expected since a material with a

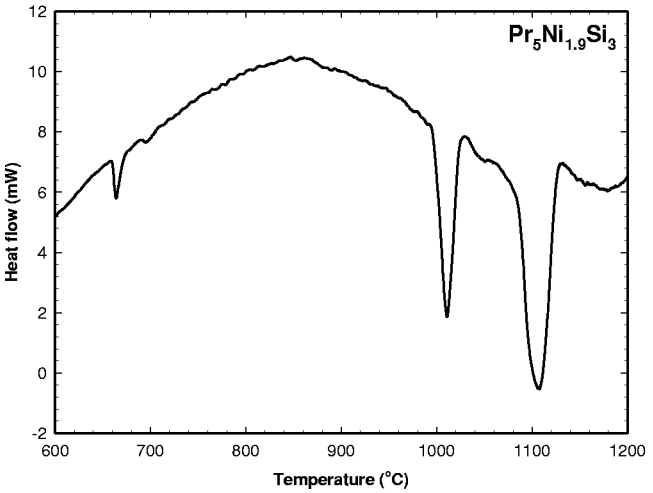

FIG. 5. The DTA trace of $Pr_5Ni_{1.9}Si_3$ measured on heating with a 10 °C/min rate. The sample for the measurements was taken from the alloy with the $Pr_5Ni_{1.9}Si_3$ stoichiometry heat treated 5 days at 600 °C.

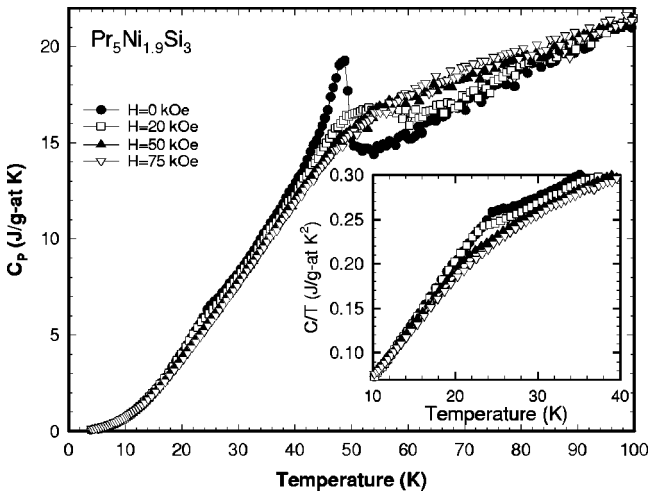

FIG. 6. The heat capacity of $Pr_5Ni_{1.9}Si_3$ from ~4 to 100 K in 0, 20, 50, and 75 kOe magnetic fields. The inset illustrates C/T over the 10–40 K temperature range to clarify the behavior of the anomaly observed at 25 K.

lower magnetic transition temperature generally has a larger MCE, all other things being equal.[17]

D. Magnetization of $Pr_5Ni_{1.9}Si_3$

Field cooling magnetization measurements of $Pr_5Ni_{1.9}Si_3$, shown in Fig. 10, were performed over the temperature range from 10 to 400 K in magnetic fields of 0.1, 1, 10, 20, 30, 40, and 50 kOe. Above 50 K, the curves for M/H vs T are identical within experimental error with the exception of the 100 Oe data. The latter deviate from the other curves by approximately 1%. The deviation may be attributed to a minor ($<0.1\%$) ferromagnetic impurity phase. The magnetic susceptibility was calculated by a linear regression fit to the magnetization values for the 1, 10, 20, 30, 40, and 50 kOe at each temperature, which in this case resulted in the same values as simply taking M/H for these fields. Above 50 K, the inverse susceptibility (Fig. 11) is approximately Curie-

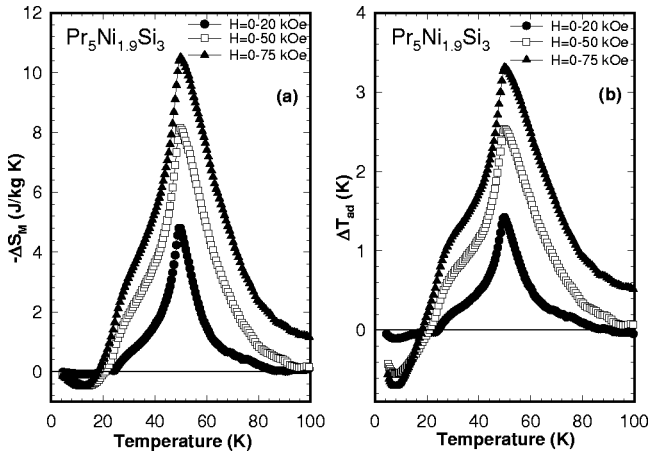

FIG. 7. The magnetic entropy change (a) and the adiabatic temperature change (b) of $Pr_5Ni_{1.9}Si_3$ calculated from heat capacity for various magnetic field changes.

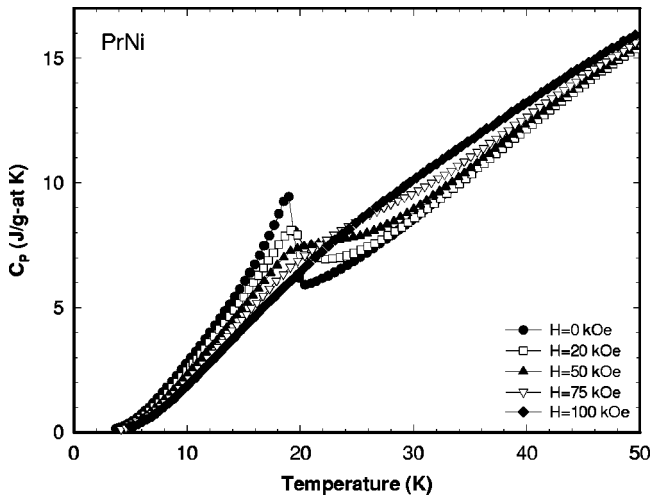

FIG. 8. The heat capacity of PrNi from ~4 to 50 K in 0, 20, 50, 75, and 100 kOe magnetic fields.

Weiss like: however, small systematic deviations from the Curie-Weiss behavior give a clear indication of crystal field effects. A least-squares fit of the data between 60 and 150 K yields a paramagnetic Curie temperature $\theta_p = 36$ K and an effective magnetic moment of $3.3\mu_B$ per Pr atom. The latter compares favorably to the theoretical value of $3.58\mu_B$.

The magnetization of $Pr_5Ni_{1.9}Si_3$ below 50 K is quite interesting. The onset of a ferromagnetic or ferrimagnetic state is evident at all fields: see Fig. 10. However, for intermediate fields the behavior of the magnetization as a function of temperature is nonmonotonic with a peak in the magnetization occurring between the ordering temperature and the lowest temperature measured. This is indicative of strong antiferromagnetic interactions, which become significant below about 25 K, confirming the heat capacity measurement: see above.

Magnetization versus field measurements at low temperature (Fig. 12) show strong evidence of competing ferromagnetic and antiferromagnetic interactions. At 25 K, the hysteresis curve for the material is typical of what is expected for a polycrystalline ferromagnet or ferrimagnet with large grains

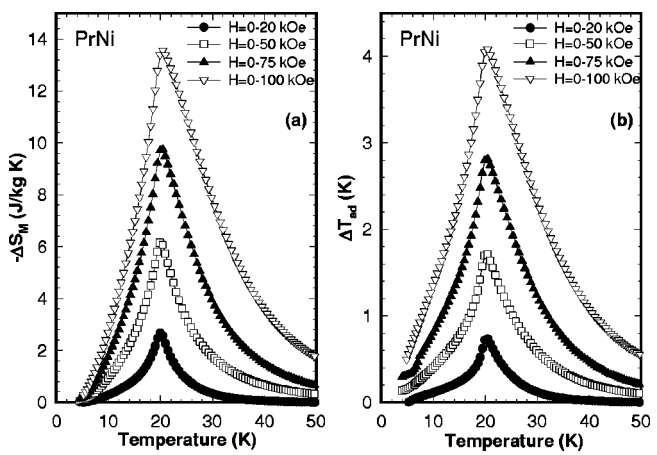

FIG. 9. The magnetic entropy change (a) and the adiabatic temperature change (b) of PrNi calculated from heat capacity for various magnetic field changes.

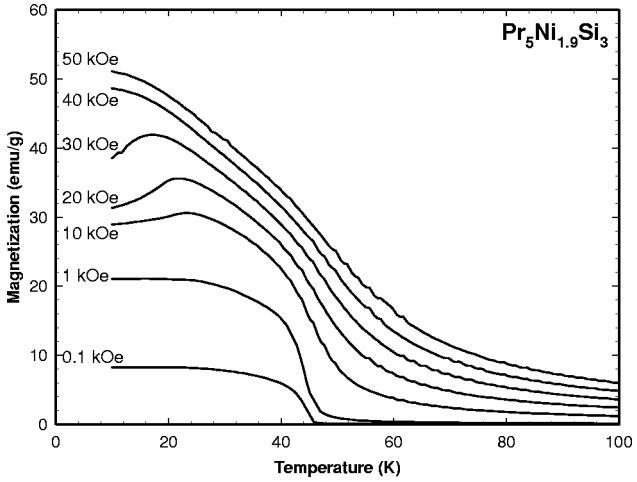

FIG. 10. Magnetization of $Pr_5Ni_{1.9}Si_3$ measured on cooling in magnetic field varying between 0.1 and 50 kOe.

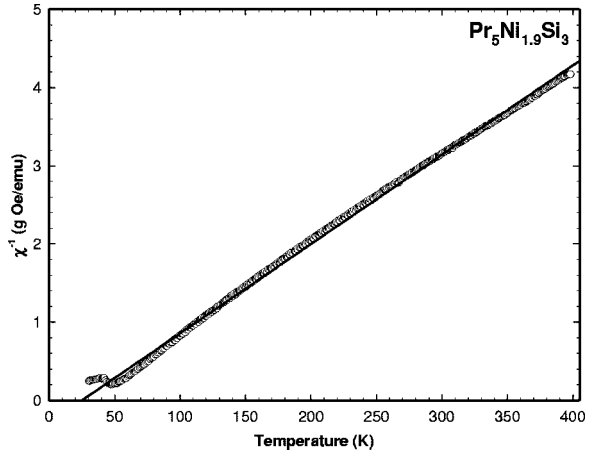

FIG. 11. Inverse magnetic susceptibility of $Pr_5Ni_{1.9}Si_3$ (symbols) and least-squares fit of the data above 50 K to the Curie-Weiss law (solid line).

and large anisotropy (the sample had randomly oriented grains, which were visible to the eye). The loop exhibits little hysteresis but the magnetization is not saturated at 5 T. Below 25 K, two significant changes occur in the loops. First, there is the development of significant coercivity, which approaches 10 kOe at 5 K. At the same time, there is evidence of a metamagnetic transition at fields around 30 kOe. Furthermore, no hysteresis is associated with the metamagentic transition. These data indicate that in low magnetic field,

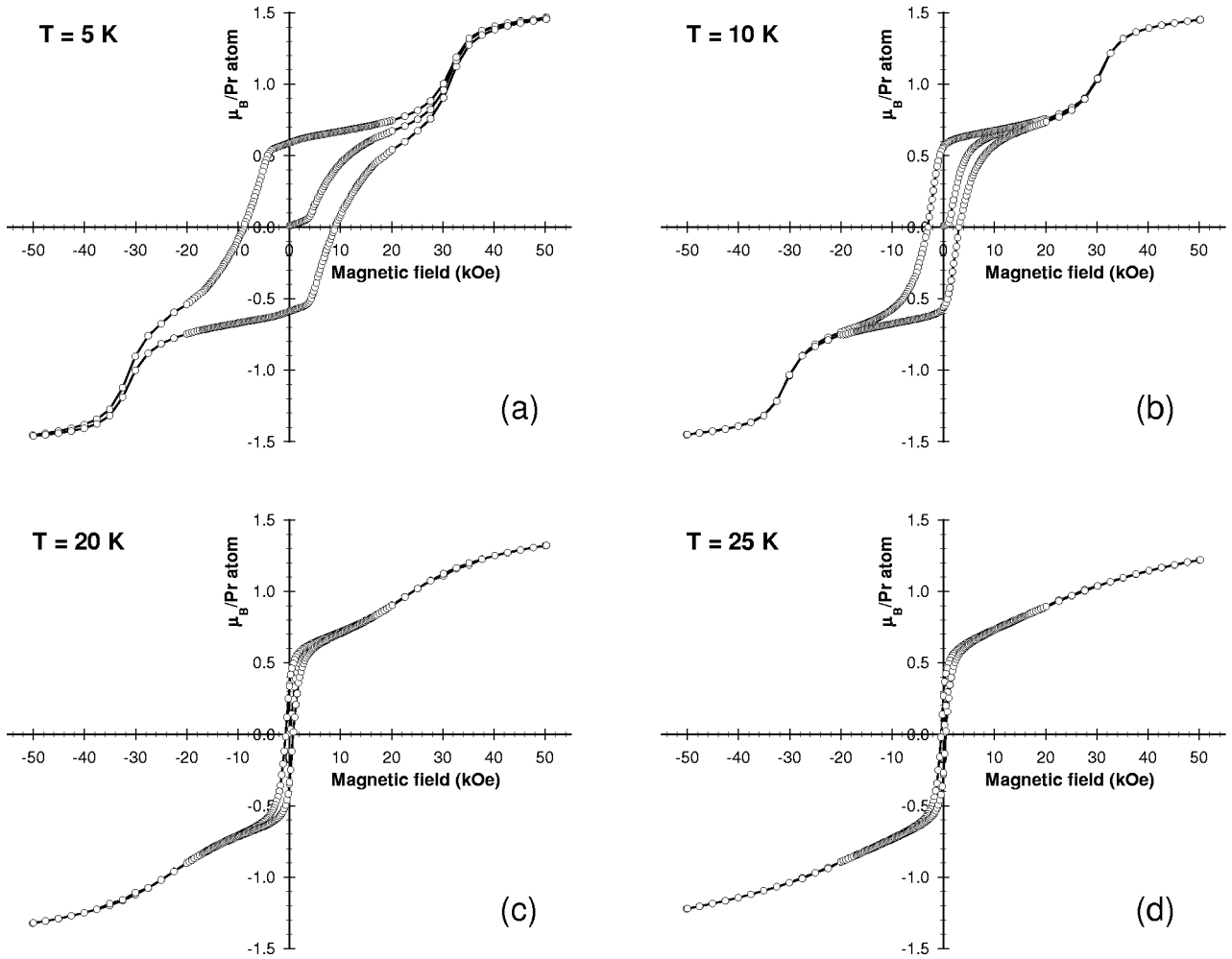

FIG. 12. Isothermal magnetization of $Pr_5Ni_{1.9}Si_3$ at 5, 10, 20, and 25 K measured using a sample cooled in zero magnetic field from ~100 K to the temperature of the measurement.

there is a transition from a low-temperature ''ferrimagnetic'' state ($T<25$ K) to a high-temperature ''ferromagnetic'' state ($25\ \mathrm{K}<T<50\ \mathrm{K}$). This transition is suppressed by magnetic fields of 20 kOe or greater. It should be noted that at no time is the full Pr moment observed below 50 kOe and the exact nature of the magnetic ordering may be quite complex with the Pr moments pointing in site-dependent directions. Given the large grain size of the sample employed in the measurements, the large hystersis at 5 K suggests that there is considerable domain wall pinning within the grains. This effect will require further study.

E. Comparison of $Pr_5Ni_{1.9}Si_3$ and PrNi

Both intermetallic compounds contain approximately 50 at. % of Pr, but as we showed above, their thermal and magnetic properties are quite different. The ternary $Pr_5Ni_{1.9}Si_3$ orders magnetically at ~ 50 K and it undergoes a ferrimagnetic transformation upon further cooling. The binary PrNi has a ferromagnetic ground state, as was established before[14] and confirmed by our heat capacity measurements. The complex behaviors of the heat capacity, the MCE, and the magnetization, exhibited by $Pr_5Ni_{1.9}Si_3$, likely reflect the complexity of its crystal structure, bonding, and exchange interactions. It is likely that the competition between ferromagnetic and antiferromagnetic ground states, as evidenced by the behavior of the physical properties of the material, is related to the differences in the interactions within and between the complex trigonal prismatic columns found in the crystal structure of $Pr_5Ni_{1.9}Si_3$. Furthermore, the distinct triangular configurations of Pr atoms create a basis for spin frustrations and, therefore, may result in a complex temperature-dependent magnetic structure of the compound.

IV. CONCLUSIONS

$Pr_5Ni_{1.9}Si_3$ belongs to a series of intermetallic compounds where chemical bonding within and between trigonal prismatic columns in a three-dimensional lattice are different and can be controlled by varying material's chemistry. The magnetization and heat capacity measurements and calculations of the magnetocaloric effect reveal a ferromagnetic ordering at 50 K and a second magnetic transition at 25 K; the latter is suppressed by magnetic fields exceeding 20 kOe. Furthermore, as inferred from the behavior of both the magnetocaloric effect and isothermal magnetization, both ferromagnetic and antiferromagnetic components are present in the magnetic ground state of the material, which is related to the specifics of its crystal structure and may result in a complex spin structure. The heat capacity and magnetocaloric effect of PrNi confirm that it orders ferromagnetically at 19 K. Both $Pr_5Ni_{1.9}Si_3$ and PrNi exhibit moderate magnetocaloric effects. The maximum MCE for $Pr_5Ni_{1.9}Si_3$ is 3.4 K and it is observed at 50 K for a magnetic field change from 0 to 75 kOe. The maximum MCE for PrNi is 4.2 K, which occurs at 19 K for a magnetic field change from 0 to 100 kOe.

ACKNOWLEDGMENTS

We thank Dr. D.C. Jiles, Dr. T.A. Lograsso, Dr. B.N. Harmon, and Dr. J.E. Snyder for useful discussions of the results presented in this work. This paper has been authored by Iowa State University of Science and Technology under Contract No. W-7405-ENG-82 with the U.S. Department of Energy. This work was supported by the Office of Basic Energy Sciences, Materials Sciences Division of the U.S. DOE.

*Electronic address: vitkp@ameslab.gov

[1] P. Rogl, in *Handbook on the Physics and Chemistry of Rare Earths*, edited by K. A. Gschneidner, Jr. and L. R. Eyring (North-Holland, Amsterdam, 1987), Vol. 7, p. 1.

[2] O. I. Bodak, E. I. Gladyshevskii, and O. I. Kharchenko, Sov. Phys. Crystallogr. **19**, 45 (1974).

[3] O. I. Bodak, E. I. Gladyshevskii, and M. G. Mis'kiv, Sov. Phys. Crystallogr. **17**, 439 (1972).

[4] E. Hovestreydt and E. Parthé, Acta Crystallogr., Sect. C: Cryst. Struct. Commun. **41**, 310 (1985).

[5] M. G. Mis'kiv, O. I. Bodak, and E. I. Gladyshevskii, Sov. Phys. Crystallogr. **18**, 450 (1974).

[6] O. I. Bodak and E. I. Gladyshevskii, *Crystallography of Intermetallic Compounds of Rare Earths* (Vyshcha Shkola, Lviv State University, Lviv, 1982).

[7] *XRD Single Crystal Software*, Bruker Analytical X-Ray System, Madison, WI, 2002.

[8] A. E. Dwight, R. A. Conner, Jr., and J. W. Downey, Acta Crystallogr. **18**, 835 (1965).

[9] O. I. Kharchenko, O. S. Koshel, and O. I. Bodak, Metallofizika (Kiev) **52**, 101 (1974).

[10] *Binary Alloy Phase Diagrams*, edited by T. B. Massalski, H. Okamoto, P. R. Subramanian, and L. Kacprzak (ASM International, Materials Park, OH, 1990).

[11] V. K. Pecharsky, J. O. Moorman, and K. A. Gschneidner, Jr., Rev. Sci. Instrum. **68**, 4196 (1997).

[12] V. K. Pecharsky and K. A. Gschneidner, Jr., J. Appl. Phys. **86**, 565 (1999).

[13] T. B. Johansson, B. Lebech, M. Nielsen, H. Moeller, H. Bjerrum, and A. R. Mackintosh, Phys. Rev. Lett. **25**, 524 (1970).

[14] G. Fillion, D. Gignoux, F. Givord, and R. Lemaire, J. Magn. Magn. Mater. **44**, 173 (1984).

[15] K. A. Gschneidner, Jr., in *Proceedings of the 9th Rare Earth Research Conference*, Virginia, 1971, edited by P. E. Field (National Technical Information Service, U.S. Department of Commerce, Springfield, VA, 1971).

[16] A. R. Mackintosh, Phys. Lett. **4**, 140 (1963).

[17] K. A. Gschneidner, Jr., V. K. Pecharsky, M. J. Gailloux, and H. Takeya, Adv. Cryog. Eng. **42**, 465 (1996).